ASSESSMENT OF SUBGRID SCALAR MIXING MODELS FOR LES OF REACTING FLOWS

Olivia S. Sun and Lester K. Su
Applied Fluid Imaging Laboratory
Department of Mechanical Engineering
The Johns Hopkins University
Baltimore, Maryland 21218 USA
osun@jhu.edu, lsu@jhu.edu

ABSTRACT

LES models for subgrid scalar dissipation are tested *a priori* using experimental data from an axisymmetric, turbulent, co-flowing jet. The models tested include: a gradient-based model, which is based on a local equilibrium assumption, a model that assumes proportionality between mechanical and scalar time scales, and a dynamic structure model based on scale-similarity ideas. Of primary interest is the structural accuracy of the models, which can be assessed by computing a correlation coefficient between exact and modeled terms. We also examine some of the fundamental assumptions underlying the models. Results suggest that assumptions of time-scale proportionality are more valid than those of local equilibrium.

INTRODUCTION

A major challenge facing large eddy simulation (LES) of reacting flows is accurate representation of the mixing process. Molecular mixing of fuel and oxidizer is the necessary precursor to chemical reaction. Since molecular mixing occurs exclusively at scales that are smaller than LES filter scales, the accuracy of subgrid mixing models is crucial. A complete description of non-premixed combustion requires accurate determination of not only resolved-scale scalar transport, but also species mixture fractions at the subgrid level. In particular, LES of reacting flows requires information on the subgrid scale (SGS) scalar dissipation. Several approaches have been taken to modeling the SGS scalar dissipation. Included among these is a gradient-based model developed using a local equilibrium assumption (Pierce and Moin, 1998), a model based on an assumption that mechanical and scalar time scales are proportional (Jimènez *et al.*, 2001), and a model based on scale-similarity ideas (Chumakov and Rutland, 2004).

Tests of these models have been few, typically using DNS data; only very limited results have been reported of tests using experimental data. Given the significance of the mixing problem, it is vital that SGS mixing models be subjected to rigorous assessment, including using experimental data. The present objective is to examine the fundamental physical assumptions in the models, and to identify major factors influencing model performance. The models are evaluated *a priori* using simultaneous planar experimental measurements of velocity and scalar mixing fields in an axisymmetric, turbulent co-flowing jet. The experiment is designed to reflect the needs of SGS model testing. The flow used is canonical and well-understood, and imaging regions are chosen to capture the jet centerline to the jet outer boundary, allowing the models to be tested across the full spatial extent of the flow. At the same time, the measurements resolve the smallest expected length scales in the scalar and velocity fields. Structural accuracy of the models is assessed by computing correlation coefficients between exact and modeled quantities. Fundamental physical assumptions are examined by analyzing spatial profiles of production and dissipation of SGS scalar variance, and of mechanical and scalar mixing time scales, to study local equilibrium and time-scale proportionality hypotheses.

SUBGRID MIXING MODELS

In LES, the transport equation for a filtered conserved scalar, $\overline{C}$, is

$$\frac{\partial \overline{C}}{\partial t} + \overline{u}_i \frac{\partial \overline{C}}{\partial x_i} - D\frac{\partial^2 \overline{C}}{\partial x_i \partial x_i} = -\frac{\partial \tau_{i,C}}{\partial x_i}, \tag{1}$$

where the overbar $\overline{(\,)}$ denotes LES filtering, D is the scalar diffusivity, and the SGS flux term $\tau_{i,C}$ is defined

$$\tau_{i,C} = \overline{u_i C} - \overline{u_i}\,\overline{C}. \tag{2}$$

This $\tau_{i,C}$ is the analog of the subgrid stress tensor for the LES-filtered Navier-Stokes equations. The term $\overline{u_i C}$ is not resolved in an LES, so $\tau_{i,C}$ must be modeled.

Analogous to the subgrid kinetic energy, $\overline{k} = (\overline{u_j u_j} - \overline{u_j}\,\overline{u_j})/2$, the subgrid "scalar energy", also referred to as the subgrid scalar variance, can be defined as

$$\theta_C \equiv \overline{C C} - \overline{C}\,\overline{C}. \tag{3}$$

This quantity in turn observes the transport equation (Jimènez *et al.*, 2001)

$$\begin{aligned}\frac{\partial \theta_C}{\partial t} + \frac{\partial \overline{u_j}\theta_C}{\partial x_j} - D\frac{\partial^2 \theta_C}{\partial x_i \partial x_i} = &\underbrace{-\frac{\partial}{\partial x_i}(\overline{u_i C^2} - \overline{u_i}\,\overline{C^2})}_{\text{I}} \\ &\underbrace{-2D\overline{\frac{\partial C}{\partial x_i}\frac{\partial C}{\partial x_i}}}_{\text{II}} + 2D\frac{\partial \overline{C}}{\partial x_i}\frac{\partial \overline{C}}{\partial x_i} \\ &\underbrace{+2\frac{\partial \overline{C}\tau_{i,C}}{\partial x_i}}_{\text{III}} \underbrace{-2\tau_{i,C}\frac{\partial \overline{C}}{\partial x_i}}_{\text{IV}}.\end{aligned} \tag{4}$$

The four unclosed terms in Eq. 4 represent turbulent convection of scalar (term I), SGS dissipation of scalar (II), large-scale diffusion (III), and production of θ_C at large scales (IV).

Terms III and IV can be closed by using models for the subgrid flux, $\tau_{i,C}$, also used for Eq. 1, and term I can be closed by using a series expansion (Chumakov and Rutland, 2004) or an appropriate model (Jimènez *et al.*, 2001). Closing the SGS scalar dissipation (term II), defined as

$$\overline{\chi} \equiv 2D\overline{\frac{\partial C}{\partial x_i}\frac{\partial C}{\partial x_i}}, \tag{5}$$

requires an additional model. For the subgrid scalar dissipation, $\overline{\chi}$, the models tested include a gradient-based model by Pierce and Moin (1998),

$$\overline{\chi} \approx 2D_t \frac{\partial \overline{C}}{\partial x_i}\frac{\partial \overline{C}}{\partial x_i}, \tag{6}$$

where D_t is a turbulent diffusivity defined as $D_t = \alpha_s \overline{\Delta}^2 |\overline{S}|$, with α_s as determined using the dynamic procedure (Germano *et al.*, 1991). This model was developed based on the assumption that, in equilibrium flow, the production of subgrid scalar variance by the resolved scales is equal in magnitude to the subgrid dissipation of scalar variance, i.e., referring to terms in Eq. 4,

$$2\tau_{i,C}\frac{\partial \overline{C}}{\partial x_i} \approx 2D\overline{\frac{\partial C}{\partial x_i}\frac{\partial C}{\partial x_i}}. \tag{7}$$

The model formulation in Eq. 6 is obtained by using an eddy diffusivity model for $\tau_{i,C}$ (Pierce and Moin, 1998).

A model for $\overline{\chi}$ proposed by Jimènez *et al.* assumes that mechanical and scalar time scales are proportional (Jimènez *et al.*, 2001). In this model, an SGS turbulent time scale is defined as

$$t = \frac{\overline{k}}{\overline{\epsilon}}, \tag{8}$$

where $\overline{k}$ is the subgrid kinetic energy and $\overline{\epsilon} = 2\nu\overline{S_{ij}S_{ij}}$ is the filtered kinetic energy dissipation rate, and an analogous SGS scalar time scale is defined as

$$t_C = \frac{\theta_C}{\overline{\chi}}, \tag{9}$$

where θ_C is the subgrid scalar variance and $\overline{\chi}$ is the subgrid scalar dissipation. Assuming proportionality between the two time scales, the proposed model reads

$$\overline{\chi} \approx \alpha_\chi \frac{\overline{\epsilon}}{\overline{k}}\theta_C. \tag{10}$$

Here, α_χ is a proportionality constant taken to be $1/Sc$. In an actual LES, neither the SGS kinetic energy, $\overline{k}$, nor the filtered kinetic energy dissipation rate, $\overline{\epsilon}$, appearing in Eq. 10 can be computed explicitly, so Jimènez *et al.* (2001) recommends that these terms be modeled as

$$\overline{\epsilon} \approx 2(\nu + \alpha_\tau \overline{\Delta}^2 |\overline{S}|)\overline{S}_{ij}\overline{S}_{ij}, \qquad \overline{k} \approx 2\alpha_I \overline{\Delta}^2 \overline{S}_{ij}\overline{S}_{ij} \tag{11}$$

with α_τ and α_I both determined using the dynamic procedure (Germano *et al.*, 1991).

The dynamic structure model for subgrid scalar dissipation reported by Chumakov and Rutland (2004) is

$$\overline{\chi}_C \approx 2D\frac{\theta_C}{\widehat{\overline{C}}\widehat{\overline{C}} - \widehat{\overline{C}}\,\widehat{\overline{C}}}\left(\widehat{\frac{\partial \overline{C}}{\partial x_i}\frac{\partial \overline{C}}{\partial x_i}} - \frac{\partial \widehat{\overline{C}}}{\partial x_i}\frac{\partial \widehat{\overline{C}}}{\partial x_i}\right). \tag{12}$$

The assumption here is that $\overline{\chi}_C$ is scale similar and that its structure can be represented by a Leonard-type term, defined here to be

$$L_{\overline{\chi}} \equiv \widehat{\frac{\partial \overline{C}}{\partial x_i}}\widehat{\frac{\partial \overline{C}}{\partial x_i}} - \frac{\partial \widehat{\overline{C}}}{\partial x_i}\frac{\partial \widehat{\overline{C}}}{\partial x_i}. \tag{13}$$

It should be noted that in this model, the subgrid scalar dissipation is defined slightly differently from Eq. 10 as

$$\overline{\chi}_C \equiv 2D\left(\overline{\frac{\partial C}{\partial x_i}\frac{\partial C}{\partial x_i}} - \frac{\partial \overline{C}}{\partial x_i}\frac{\partial \overline{C}}{\partial x_i}\right). \tag{14}$$

EXPERIMENTAL DATA

The experimental data used here are from simultaneous, planar measurements of velocity and scalar fields in an axisymmetric, turbulent, co-flowing jet. The co-flow consists of air, seeded with a glycerol-water fog, while the jet consists of air, seeded with acetone vapor to 23% by volume for diagnostic purposes. The Schmidt number is $Sc = 1.49$. Two sets of data are taken at different jet exit Reynolds numbers, $Re = 1800$ and $Re = 5600$, with downstream locations spanning $x/D = 30$ to $x/D = 35$. The imaging regions are chosen to span from $r = 0$ to $r = \delta/2$ (from the jet centerline to the outer boundary). Here, $\delta = \delta_{0.05}$ is defined as the full width of the jet velocity profile at 5% of maximum.

Particle image velocimetry (PIV) is used to measure the velocity fields and planar laser-induced fluorescence (PLIF) is used to measure the scalar field. The light source is a single, dual cavity Nd:YAG laser (Spectra-Physics PIV-400) with 532 nm output, 93% of which is further frequency-doubled to generate the 266 nm output for the PLIF measurements, with the remaining 7% used for the PIV measurements. A total of 1000 imaging planes, each with a 1392x1040 pixel PIV image resolution and 325x257 pixel PLIF image resolution, were used. The PIV images are processed using a cross-correlation algorithm incorporating multi-grid, iterative interrrogation window offset and deformation to improve vector yield and resolution. The smallest interrogation windows used span 16x16 pixels, giving a final velocity field resolution of 163x119 pixels. The grid spacing, $\Delta x = 185$ μm, was smaller than the estimated finest scales of velocity and scalar fields, $\lambda_\nu = 440$ μm and $\lambda_D = 360$ μm, throughout the measurement windows. Here, λ_ν and λ_D are defined as (e.g. Su and Mungal, 2004)

$$\lambda_\nu \equiv 10\ \delta\ Re_\delta^{-3/4}, \text{ and} \tag{15}$$

$$\lambda_D \equiv \lambda_\nu\ Sc^{-1/2} \tag{16}$$

defined in terms of the local outer-scale Reynolds number

$$Re_\delta = U_c(x)\delta/\nu, \tag{17}$$

where $U_c(x)$ is the mean jet centerline velocity.

RESULTS

The SGS models are evaluated *a priori* by filtering the resolved experimental data to emulate LES data and applying the models to the filtered data. The quality of the models is assessed through correlations between the modeled and measured values. The correlation coefficient, r, measures the validity of the basic modeling assumptions, by quantifying the degree to which the structure of $\overline{\chi}$ is captured by the models.

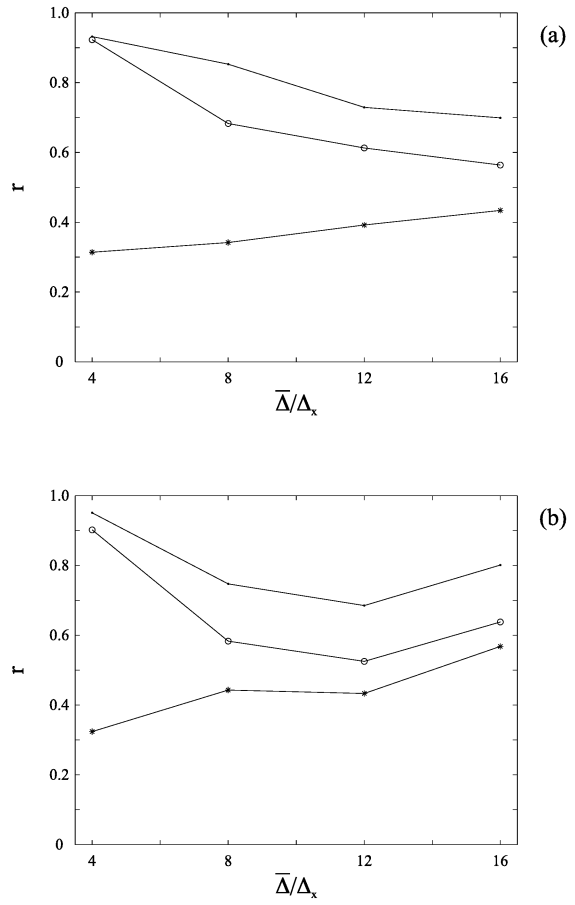

Figure 1: Correlation between modeled vs. exact terms at (a) $Re = 1800$ and (b) $Re = 5600$ for the Jimènez ($\cdot$), gradient ($*$), and dynamic structure ($\circ$) models.

Figure 1 summarizes the correlation results for the scalar dissipation models Eqs. 6, 10 and 12 at $Re = 1800$ and 5600, respectively. The gradient-based model (Eq. 6) is found to have the lowest correlations at all grid filter sizes, while the Jimènez model has the highest correlation for all grid filter sizes. The dynamic structure model has correlation values comparable to that of the Jimènez (2001) model. With the exception of the largest grid filter size, $\overline{\Delta} = 16\Delta_x$, each model had similar correlation values at the different Reynolds numbers, for each filter width. While model performance is only slightly affected by the change in Re, it appears that there is a larger dependency on grid filter width. The results presented here differ slightly from those reported previously (Sun and Su, 2004). In particular, the dynamic structure model has higher correlations compared to previous results (Sun and Su, 2004). The cause for this discrepancy is not completely understood; however, in both the previous study as well as this current work, it is evident that assessment of model performance is quite sensitive to both measurement resolution and statistical convergence. The measurements used here have superior resolution, and because the number of imaging planes used is more than twice that of the previous work, it is reasonable to assume that the statistics here are better converged.

As mentioned previously, the gradient-based model for $\overline{\chi}$ by Pierce and Moin (1998) is based on the assumption that production of subgrid scalar variance, θ_C, is in equilibrium with SGS scalar dissipation, $\overline{\chi}$. Mean radial profiles of the production of SGS scalar variance, p, defined as

$$p \equiv 2\tau_{i,C}\frac{\partial \overline{C}}{\partial x_i}, \tag{18}$$

and of $\overline{\chi}$, for different grid filter sizes are shown in Figure 2. The data are averaged along lines of fixed r/δ in the downstream direction over all available image planes. The dissipation, $\overline{\chi}$, is rescaled in the figure by an appropriate constant for comparison purposes. Profiles for p and $\overline{\chi}$ are not found to have similar shapes, and magnitudes of the two quantities differ noticeably. The large discrepancy in magnitude and shape between the profiles of p and $\overline{\chi}$ may explain the overall poorer correlations obtained using the gradient-based model (Eq. 6) for $\overline{\chi}$ compared to the other two models (Eqs. 10 and 12). The magnitude of p appears to be filter size dependent, and increases with increasing filter size, while the magnitude of $\overline{\chi}$ remains nearly constant for all filter sizes used. This result is not unexpected, since the production of subgrid scalar variance by definition (Eq. 18) includes resolved-scale quantities that may be filter dependent. On the other hand, the subgrid scalar dissipation, $\overline{\chi}$, is largely dominated by unresolved, sub-filter scales and should not be strongly affected by filter size. Therefore, as seen in Figure 2, the quality of the local equilibrium assumption (Eq. 7) becomes worse with increasing filter size, as the differences in magnitude and shape between the production and dissipation profiles become larger. This result is at odds with the results shown in Figure 1, where the correlations for the gradient model tend to increase with increasing filter size. This suggests that the model performance, as measured by a correlation coefficient, is not affected solely by the quality of the underlying local equilibrium assumption.

The dissipation model presented by Jimènez *et al.* (2001) is based on the assumption that mechanical and scalar time scales are proportional, i.e. $t/t_C \approx \beta$, where β is some constant. In a previous study, Bèguier *et al.* (1978) found experimentally that $\beta \approx 0.5$. However, others have found very different values for β, which suggests β may be dependent on flow parameters and cannot be taken as universal (Sanders and Gokalp, 1997, Panchapakesan and Lumley, 1993). Figure 3 presents mean radial profiles of t/t_C for different grid filter sizes. The ratio is close to the value of 0.5 found by Bèguier *et al.* (1978) for the smallest grid filter size, $\overline{\Delta} = 4\Delta_x$ and decreases to values of 0.3 for the largest grid filter size, $\overline{\Delta} = 16\Delta_x$. It is evident that the time scale ratio changes in magnitude with different filter sizes as well as with Reynolds number, but that its profile maintains a consistent shape, and, additionally, remains fairly constant across the width of the jet. From Eq. 10, the assumption $\alpha_\chi = 1/Sc$ implies that the time scale ratio, t/t_C, should obey the relation $t/t_C \approx 1/Sc$, which, in this study, is $t/t_C \approx 0.67$. Results in Fig. 3 show that t/t_C is less than the expected value $1/Sc$ for all cases considered here. However, the relative consistency of t/t_C in the radial direction indicates that the time-scale proportionality approximation, Eq. 10, is acceptable for a majority of the flow regime. This observation is perhaps reflected in the high correlation values obtained with the Jimènez model.

To examine further the relationship between the observed spatial profiles of production, dissipation, and time-scale ratio, the flow was divided into two regions, labeled as region I, which

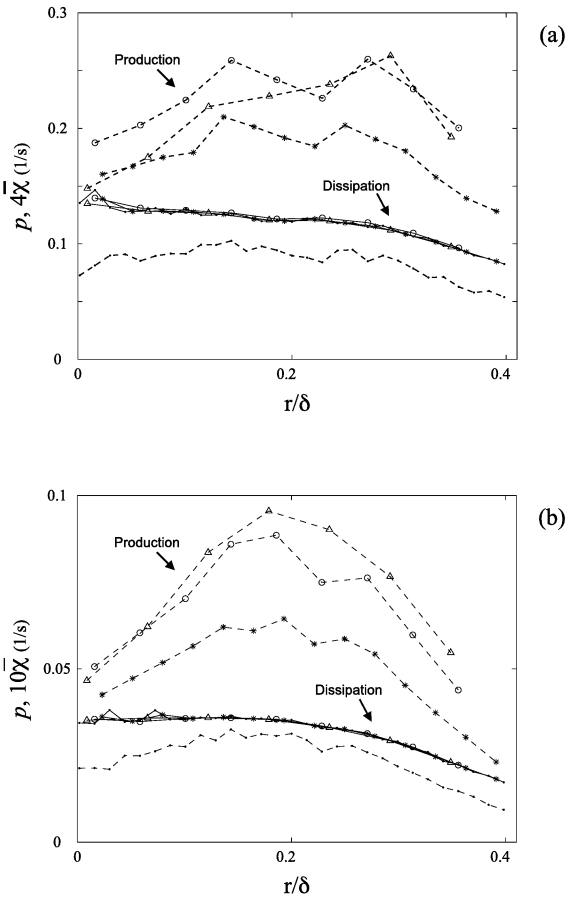

Figure 2: Mean profiles of SGS production ($--$) and dissipation ($-$) for different grid filter sizes, $\overline{\Delta} = 4$ ($\cdot$), $\overline{\Delta} = 8$ ($*$), $\overline{\Delta} = 12$ ($\circ$), $\overline{\Delta} = 16$ ($\triangle$), at (a) $Re = 1800$ and (b) $Re = 5600$. $\overline{\chi}$ is rescaled by an appropriate constant for comparison purposes.

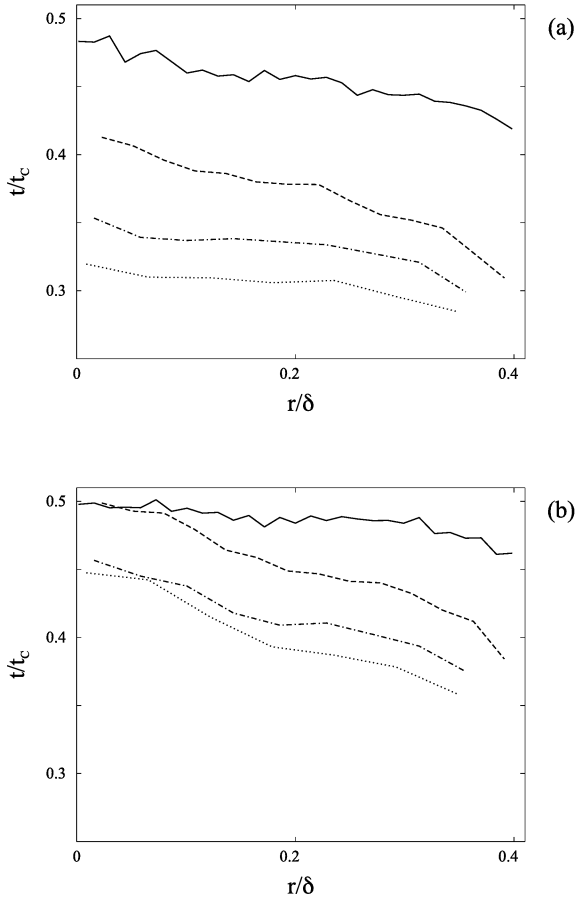

Figure 3: Mean profiles of t/t_C for different grid filter sizes $\overline{\Delta} = 4$ ($-$), $\overline{\Delta} = 8$ ($--$), $\overline{\Delta} = 12$ ($-\cdot$), $\overline{\Delta} = 16$ ($\cdot\cdot$) at (a) $Re = 1800$ and (b) $Re = 5600$.

corresponds to $0 < r/\delta < 0.2$, where $r = 0$ is the jet centerline, and region II, which corresponds to $0.2 < r/\delta < 0.4$. Correlation coefficients between modeled and exact values were then computed using only data points within the particular regions. The regions were chosen based on the observed changes in the mean radial profiles (Figs. 2 and 3), as well as the need to ensure statistical convergence in each region. The results are summarized in Tables 1 and 2. It can be seen that the gradient model (Eq. 6) is most sensitive to this type of conditional correlation, as the correlation values for this model differ by up to 100%, depending on the region of the flow used in the calculation. For both Re cases, the gradient model has higher correlations in region II, the outside region of the jet, compared to region I. The reason for this result is not yet clear. However, from Fig. 2 it appears that the radial profiles of production and dissipation are more similar in shape further away from the jet centerline, which may explain the higher correlations observed for the gradient model in region II. It remains unclear how this relates to the correlation versus filter size results in Figure 1.

It is interesting that profiles of mechanical-to-scalar time scale ratio (Fig. 3) show that t/t_C is more uniform, and closer in magnitude to the expected value $1/Sc = 0.67$, near the jet centerline, and decreases in the outer regions of the jet. It is therefore expected that the Jimènez model would perform better in region I, where the approximation $t/t_C \approx 1/Sc$ is more valid. However, as seen in Tables 1 and 2, the Jimènez model, like the gradient model, has higher correlations in region II, near the outside of the jet, than in region I.

These preliminary observations based on conditional statistics suggest that additional factors may affect the validity of the models beyond the underlying physical assumptions of local equilibrium and time scale proportionality. For example, it is known that both subgrid scalar variance, θ_C, and subgrid scalar dissipation, $\overline{\chi}$, decrease away from the centerline of the jet, possibly affecting the accuracy of the assumptions and the models. These results also point to the complexity of assessing model performance.

CONCLUSIONS

Subgrid scale models for subgrid scalar dissipation rate are studied using experimental data from an axisymmetric, turbulent jet. The models examined include a gradient-based model (Pierce and Moin, 1998), which is based on a local equilibrium assumption, a model by Jimènez *et al.* (2001), which assumes proportionality between mechanical and scalar time scales, and a dynamic structure model (Chumakov and Rutland,

Model	$\overline{\Delta}$	r_{I}	r_{II}
Gradient	$4\,\Delta_x$	0.312	0.796
	$8\,\Delta_x$	0.328	0.754
	$12\,\Delta_x$	0.380	0.730
	$16\,\Delta_x$	0.463	0.710
Jimènez	$4\,\Delta_x$	0.912	0.976
	$8\,\Delta_x$	0.871	0.948
	$12\,\Delta_x$	0.735	0.914
	$16\,\Delta_x$	0.726	0.904
Dynamic Structure	$4\,\Delta_x$	0.910	0.780
	$8\,\Delta_x$	0.695	0.765
	$12\,\Delta_x$	0.571	0.720
	$16\,\Delta_x$	0.536	0.755

Table 1: Correlation coeffcients for $\overline{\chi}$ at $Re = 1800$ for different spatial regions in the flow. Region I corresponds to $0 < r/\delta < 0.2$, Region II corresponds to $0.2 < r/\delta < 0.4$.

Model	$\overline{\Delta}$	r_{I}	r_{II}
Gradient	$4\,\Delta_x$	0.301	0.789
	$8\,\Delta_x$	0.660	0.736
	$12\,\Delta_x$	0.643	0.689
	$16\,\Delta_x$	0.617	0.681
Jimènez	$4\,\Delta_x$	0.985	0.965
	$8\,\Delta_x$	0.903	0.933
	$12\,\Delta_x$	0.874	0.903
	$16\,\Delta_x$	0.851	0.888
Dynamic Structure	$4\,\Delta_x$	0.936	0.704
	$8\,\Delta_x$	0.699	0.734
	$12\,\Delta_x$	0.668	0.697
	$16\,\Delta_x$	0.657	0.693

Table 2: Correlation coeffcients for $\overline{\chi}$ at $Re = 5600$ for different spatial regions in the flow. Region I corresponds to $0 < r/\delta < 0.2$, Region II corresponds to $0.2 < r/\delta < 0.4$.

2004) based on scale-similarity ideas. Of these models, the model by Jimènez *et al.* (1998) gives the highest correlation coefficients between modeled and exact quantities for all grid filter sizes tested. Examining radial profiles of mechanical-to-scalar time scale ratio, it is evident that the ratio t/t_C is fairly constant across the width of the jet and close in magnitude to the expected value of $1/Sc$ proposed by Jimènez *et al.* (1998). The dynamic structure model (Chumakov and Rutland, 1998) was found to have correlations comparable to the Jimènez model. The gradient-based model (Pierce and Moin, 1998) had the lowest correlations of the models tested. All models were found to vary slightly in performance at different Reynolds numbers, however, the dependency of performance on grid filter width is the more dominant of the two factors. Radial profiles of subgrid production and dissipation of scalar variance were found to be different in profile shape and magnitude, demonstrating the need to examine the local equilibrium hypothesis, Eq. 6 in more detail. Preliminary conditional correlations suggest that poor correlations between modeled and exact values of $\overline{\chi}$ may be related to regions where the assumption made in Eq. 6 is not as valid. Currently, additional detailed experiments are planned. Measurements at a larger range of Reynolds numbers and different downstream distances from the jet exit will be used to provide more comprehensive statistical analyses of factors influencing SGS model behavior.

ACKNOWLEDGEMENTS

This work is supported by the National Science Foundation. The authors thank Mr. Cody Brownell at Johns Hopkins University for his help with data collection.

REFERENCES

Beǵuier, C., Dekeyser, I., and Launder, B.E., 1978, "Ratio of scalar and velocity dissipation time scales in shear flow turbulence," *Phys. Fluids*, Vol. 21, pp. 307-310.

Chumakov, S. and Rutland, C. J., 2004, "Dynamic structure models for subgrid scalar flux and dissipation in large eddy simulation," *AIAA J.*, Vol.42, pp. 1132-1138.

Cook, A. W., and Riley, J. J., 1994, "A subgrid model for equilibrium chemistry in turbulent flows," *Phys. Fluids*, Vol. 6, pp. 2868-2870.

Germano, M., Piomelli, U., Moin, P., and Cabot, W. H., 1991, "A dynamic subgrid-scale eddy viscosity model," *Phys. Fluids*, Vol. 3, pp. 1760-1765.

Jimènez, C., Ducros, F., Cuenot, B. and Bédat, B., 2001, "Subgrid scale variance and dissipation of a scalar field in large eddy simulations," *Phys. Fluids*, Vol. 13, pp.1748-1754.

Jimènez, C., Valino, L., and Dopazo, C., 2001, "*A priori* and *a posteriori* tests of subgrid scale models for scalar transport", *Phys. Fluids*, Vol. 13, pp. 2433-2436.

Liu, S., Meneveau, C., and Katz, J., 1994, "On the properties of similarity subgrid-scale models as deduced from measurements in a turbulent jet," *J. Fluid Mech.*, Vol. 275, pp. 83-119.

Panchapakesan, N. R., and Lumley, J. L., 1993, "Turbulence measurements in axisymmetric jets of air and helium. Part 2. Helium jet," *J. Fluid Mech.*, Vol. 246, pp. 225-247.

Pierce, C. and Moin, P., 1998, "A dynamic model for subgrid-scale variance and dissipation rate of a conserved scalar," *Phys. Fluids*, Vol. 10, pp. 3041-3044.

Sanders, J. P. H., and Gokalp, I., 1997, "Scalar dissipation rate modelling in variable density turbulent axisymmetric jets and diffusion flames," *Phys. Fluids*, Vol. 10, pp. 938-948.

Su, L. K., and Clemens, N. T., 2003, "The structure of fine-scale scalar mixing in gas-phase planar turbulent jets," *J. Fluid Mech.*, Vol. 488, pp. 1-29.

Su, L. K., and Mungal, M. G., 2004, "Simultaneous measurement of scalar and velocity field evolution in turbulent crossflowing jets," *J. Fluid Mech.*, Vol. 513, pp. 1-45.

Sun, O. and Su, L. K., 2004, "Experimental assessment of scalar mixing models for large-eddy simulation," *34th AIAA Fluid Dynamics Conference and Exhibit*, Portland, OR.